Radiology

Robot-assisted Radical Prostatectomy: Multiparametric MR Imaging–directed Intraoperative Frozen-Section Analysis to Reduce the Rate of Positive Surgical Margins[1]

Giuseppe Petralia, MD
Gennaro Musi, MD
Anwar R. Padhani, MB, BS, FRCR, FRCP
Paul Summers, PhD
Giuseppe Renne, MD
Sarah Alessi, MD
Sara Raimondi, PhD
Deliu V. Matei, MD, PhD
Salvatore L. Renne, MD
Barbara A. Jereczek-Fossa, MD, PhD
Ottavio De Cobelli, MD
Massimo Bellomi, MD

Purpose: To investigate whether use of multiparametric magnetic resonance (MR) imaging–directed intraoperative frozen-section (IFS) analysis during nerve-sparing robot-assisted radical prostatectomy reduces the rate of positive surgical margins.

Materials and Methods: This retrospective analysis of prospectively acquired data was approved by an institutional ethics committee, and the requirement for informed consent was waived. Data were reviewed for 134 patients who underwent preoperative multiparametric MR imaging (T2 weighted, diffusion weighted, and dynamic contrast-material enhanced) and nerve-sparing robot-assisted radical prostatectomy, during which IFS analysis was used, and secondary resections were performed when IFS results were positive for cancer. Control patients (n = 134) matched for age, prostate-specific antigen level, and stage were selected from a pool of 322 patients who underwent nerve-sparing robot-assisted radical prostatectomy without multiparametric MR imaging and IFS analysis. Rates of positive surgical margins were compared by means of the McNemar test, and a multivariate conditional logistic regression model was used to estimate the odds ratio of positive surgical margins for patients who underwent MR imaging and IFS analysis compared with control subjects.

Results: Eighteen patients who underwent MR imaging and IFS analysis underwent secondary resections, and 13 of these patients were found to have negative surgical margins at final pathologic examination. Positive surgical margins were found less frequently in the patients who underwent MR imaging and IFS analysis than in control patients (7.5% vs 18.7%, P = .01). When the differences in risk factors are taken into account, patients who underwent MR imaging and IFS had one-seventh the risk of having positive surgical margins relative to control patients (adjusted odds ratio: 0.15; 95% confidence interval: 0.04, 0.61).

Conclusion: The significantly lower rate of positive surgical margins compared with that in control patients provides preliminary evidence of the positive clinical effect of multiparametric MR imaging–directed IFS analysis for patients who undergo prostatectomy.

© RSNA, 2014

Online supplemental material is available for this article.

Robot-assisted radical prostatectomy (RARP) has become the dominant surgical approach for treatment of prostate cancer in the United States (1) and was expected to account for more than 80% of all radical prostatectomies performed in 2013 (2). RARP facilitates nerve-sparing procedures with less damage to sexual function (3), and nerve-sparing RARP may yield better postoperative continence and potency (4). However, sparing the neurovascular bundles reduces the safety distance between cancerous tissue and surgical margins, and thus, nerve-sparing RARP may lead to higher rates of surgical margins that are positive for cancer (positive surgical margins) (5–8). Positive surgical margins can negatively affect patient outcomes, independent of extracapsular disease status (9). Therefore, the surgeon must balance the desire to minimize postoperative morbidity afforded by a nerve-sparing approach with the need to gain tumor control by avoiding positive surgical margins.

Intraoperative frozen-section (IFS) analysis is an attractive means of reducing the prevalence of positive surgical margins because it enables real-time histologic assessment of the surgical margins during nerve-sparing radical prostatectomy. The technique of IFS analysis involves cutting sections from the removed prostate that are then frozen, stained, and subjected to microscopic examination. Although IFS analysis can be performed on the whole surface of the prostate (10), it usually is performed on the posterolateral aspects of the gland to provide information on the presence or lack of involvement of the neurovascular bundle. However, IFS analysis has been criticized because of the time and costs involved, its low sensitivity and specificity, and the potentially conflicting oncologic results that have been reported (11–13). Despite these concerns, authors of a recent article (14) investigating 11 069 consecutive patients showed that the patients who underwent systematic IFS analysis of the posterolateral aspects of the gland during radical prostatectomy had a significantly lower rate of positive surgical margins (15% vs 22%, $P <$ .0001) compared with a matched group of control patients who underwent radical prostatectomy without IFS analysis.

Despite only modest improvements in staging (15), multiparametric magnetic resonance (MR) imaging, which combines T2-weighted, diffusion-weighted, and dynamic contrast material–enhanced imaging (16,17), has improved significantly the ability to depict the intraprostatic location of clinically significant cancers (> 0.5 mL, > Gleason score 6) (18–20). These larger volume index lesions are responsible for almost all positive surgical margins (21,22). In light of the promising reports for multiparametric MR imaging to show the anatomic location of dominant intraprostatic lesions and of the ability of IFS to reduce the rate of positive surgical margins in separate analyses, we hypothesized that the use of multiparametric MR imaging findings to direct IFS analysis to radiologic sites that are highly suspicious for tumor contact with the prostatic capsule would improve the oncologic outcomes compared with the standard practice for nerve-sparing RARP, which includes neither preoperative MR imaging nor IFS analysis. Thus, the purpose of our study was to investigate whether the use of multiparametric MR imaging–directed IFS analysis reduces the rate of positive surgical margins in patients undergoing nerve-sparing RARP.

Materials and Methods

This retrospective analysis of prospectively acquired data was approved by our institutional ethics committee, who waived the requirement for informed consent specific to the study because all patients provided written informed consent for MR imaging, surgical procedures, and research use of their medical information.

Patients

Five hundred eighty-two consecutive patients underwent nerve-sparing RARP at our institution between January 2010 and May 2012. Inclusion criteria for our study were the accepted criteria for nerve-sparing RARP: tumor stage 1 or 2, prostate-specific antigen (PSA) level of less than 20 ng/mL (<20 μg/L), age of 75 years or younger, and Gleason score of less than 8. Exclusion criteria were failure to meet the above inclusion criteria (for some patients who underwent elective

Advances in Knowledge

- Positive surgical margins were found less frequently at prostatectomy in patients who underwent MR imaging–directed intraoperative frozen-section (IFS) analysis than in control patients matched for age, prostate-specific antigen level, and stage (7.5% vs 18.7%, P = .01).

- Multiparametric MR imaging–directed IFS analysis resulted in one-seventh the risk of positive surgical margins than that in patients who did not undergo multiparametric MR imaging–directed IFS analysis (odds ratio: 0.15; 95% confidence interval: 0.04, 0.61).

Implication for Patient Care

- Multiparametric MR imaging–directed IFS analysis reduces rates of positive surgical margins at nerve-sparing robot-assisted laparoscopic radical prostatectomy.

nerve-sparing RARP procedures) or surgery performed by a surgeon with experience performing fewer than 150 RARP procedures. A total of 121 exclusions were made on the following bases: three for patients with tumor stage greater than 2, 13 for a PSA level greater than 20 ng/mL (>20 μg/L), four for age older than 75 years, 27 for Gleason scores of greater than or equal to 8, 69 exclusions for surgeon experience, and five for two or more exclusion criteria, resulting in a study population of 461 patients.

Between March 2011 and May 2012, 139 of these 461 patients underwent multiparametric MR imaging and 134 (mean age, 61.2 years; range, 47–73 years) completed the multiparametric MR imaging–directed IFS analysis during the nerve-sparing RARP procedure (MR imaging and IFS patient group). Reasons for noncompletion of multiparametric MR imaging–directed IFS analysis were motion artifacts on the MR images ($n = 2$), logistical difficulties for IFS analysis ($n = 2$), or an intraoperative decision to forgo IFS analysis and proceed directly to neurovascular bundle resection ($n = 1$). Assignment to the MR imaging and IFS patient group was determined on the basis of the availability of the MR imager at the time of scheduling the nerve-sparing RARP procedure, without knowledge of the clinical details of the patient.

From the remaining 322 patients who underwent nerve-sparing RARP with neither multiparametric MR imaging nor IFS analysis between January 2010 and May 2012, a contemporaneous control group of 134 patients matched for age, PSA level, and tumor stage was selected as described in Appendix E1 (online) (Fig 1).

Multiparametric MR Imaging Technique

MR imaging and IFS patients underwent multiparametric MR imaging of the prostate with a 1.5-T MR imager (Avanto; Siemens Medical Solutions, Erlangen, Germany), with an eight-channel phased-array coil. An endorectal coil was not used. The pulse sequences used were sagittal, coronal, and axial T2-weighted; axial diffusion-weighted; and axial dynamic
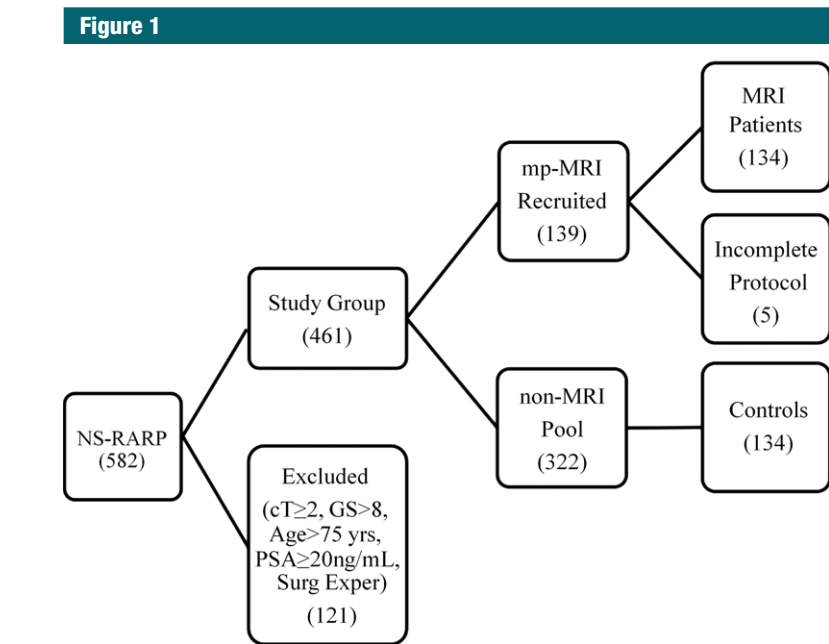
Figure 1

Figure 1: Diagram shows patient selection for multiparametric MR imaging–directed IFS analysis during nerve-sparing RARP procedure and matched control patients who underwent RARP without MR imaging–directed IFS analysis. *NS* = nerve sparing, *mp* = multiparametric, *cT* = clinical, *GS* = Gleason score.

contrast-enhanced imaging obtained before, during, and after injection of gadopentetate dimeglumine (Magnevist; Bayer Healthcare, Berlin, Germany) administered at a dose of 0.1 mmol per kilogram of body weight through a peripheral vein at a flow rate of 3 mL/sec followed by a saline bolus of 10 mL administered at the same flow rate by using a mechanical injector (Spectris MR Injection System; Medrad, Leverkusen, Germany). Imaging parameters are detailed in Table 1.

Multiparametric MR Imaging Analysis

Multiparametric MR imaging of the prostate was introduced in our institution after practitioners underwent a training period that included working with an expert in multiparametric MR imaging (A.R.P., with more than 10 years of experience). A combined reading of images from all pulse sequences was performed prospectively by two radiologists in consensus (G.P. and S.A., with 2 years and 1 year of experience, respectively, in multiparametric MR imaging of the prostate at the start of the study). Each lesion was

scored on a 1–5 scale for its appearance on T2-weighted, diffusion-weighted, and dynamic contrast-enhanced images, and a final Likert score, which was not a mathematical combination of the scores collected for each pulse sequence but a subjective final judgment on the likelihood of the presence of a clinically significant intraprostatic cancer on a 5-point scale, as recommended in previous studies (23,24): score 1, highly unlikely; score 2, unlikely; score 3, equivocal; score 4, likely; and score 5, highly likely. To arrive at the final Likert score, we gave more weight to the apparent diffusion coefficient for lesions in the peripheral zone, although the T2-weighted appearance was given more weight for lesions of the transition zone and anterior fibromuscular stroma, in keeping with evidence at the time of starting the study that both dynamic contrast-enhanced and diffusion-weighted imaging may have false-positive results because of the difficulty of discriminating prostate cancer from benign prostate hyperplasia (25), which often shows hypervascularity (26) and low apparent diffusion coefficients (27).

Table 1

Multiparametric MR Imaging Acquisition Parameters

Parameter	T2 Weighted	Diffusion Weighted	Dynamic T1-weighted Contrast Enhanced*
Acquisition plane	Axial, coronal, sagittal	Axial	Axial
Pulse sequence type	Turbo spin echo	Echo planar	Three-dimensional gradient echo
Turbo factor	23	60	. . .
b values (sec/mm^2)	. . .	0, 500, 1000	. . .
Section thickness	3	4	4
Intersection gap	0.3	0.4	0
No. of sections	18	20	20†
Acquisition duration (min:sec)	5:17	3:03	4:10
Phase-encoding direction	Right-left, right-left, anterior-posterior‡	Anterior-posterior	Anterior-posterior
Field of view (mm)	190 × 190	290 × 200	280 × 254
Acquisition matrix	320 × 320	128 × 66	320 × 228
No. of repetitions	5	8	1, 25 dynamic
Repetition time (msec)	4440	3100	7.3
Echo time (msec)	114	69	4.7
Flip angle (degrees)	90	90	25
Bandwidth (Hz/pixel)	140	1562	430

* Contrast agent (gadopentetate dimeglumine, 0.1 mmol per kg) was injected after the third dynamic acquisition at a flow rate of 3 mL/sec.

† Interpolated from reference 12.

‡ Phase-encoding directions for T2-weighted imaging are for axial, coronal, and sagittal sequences, respectively.

If one or more of the three pulse sequences indicated contact of the lesion with the prostatic capsule, the location of the lesion was indicated on a coronal and three-level axial scheme that was incorporated into a software application designed for this purpose (Radcommunicator; Orobix, Bergamo, Italy). A written report and completed graphical reporting scheme were delivered to the urologist before the nerve-sparing RARP (Fig 2).

Surgery

All procedures (for both study groups) were performed by one of three surgeons (G.M., D.V.M., and O.D.C., each with 4 years of experience, having performed more than 150 RARP procedures at the start of the study). Our institutional approach to nerve-sparing RARP is based on the technique described in Patel et al (28) that includes use of the da Vinci surgical robot system (S model; Intuitive Surgical, Sunnyvale, Calif) and a port device (Alexis; Applied Medical, Rancho Santa Margarita, Calif) system (29) (Appendix E1 [online]).

For MR imaging and IFS patients, after the prostate was removed, the surgeon marked its surface by using a dermographic pen in the area or areas where multiparametric MR imaging indicated contact of the index lesion with the prostatic capsule (Fig 2), and each area was subjected to IFS analysis. IFS analyses in which tumor cells were found in contact with the prostatic capsule were considered positive, and the tissue adjacent to this area was subjected to a secondary resection, including a partial resection of the neurovascular bundle if this area was on a posterolateral aspect of the prostate. The secondary resection tissue was also inked to indicate its orientation (apex-base, inner-outer) and subjected to a further IFS analysis of the margins. If tumor cells were found in the outer surface of the secondary resection tissue, further resections were performed. If the secondary resection was in proximity of a neurovascular bundle, the entire ipsilateral neurovascular bundle was removed, otherwise resections continued to the greatest anatomic limit possible or until negative margins were obtained.

Pathologic Evaluation

Prostate and secondary resection tissue samples were evaluated by senior

pathologists who were under the supervision of a urologic pathologist (G.R., with 20 years of experience). The tissues for IFS analysis were prepared (Appendix E1 [online]) for staining with hematoxylin and eosin for microscopic examination. The IFS procedure required an average of 30 minutes in the pathology laboratory. The samples used for IFS analysis and the prostate specimen were then fixed in formalin and were analyzed later in accordance with standard procedures for the final pathologic report (30).

Tumors were graded according to the Gleason system (31), and pathologic stage was assigned by using the 2009 TNM classification system (32). The surgical margins were reassessed with the extension of any positive surgical margins determined according to the criteria of the prostate consensus working group (33).

Statistical Analysis

A sample size calculation was performed before patient recruitment assuming a two-sided Z test with pooled variance. On the basis of prior reports (14,18–20), we hypothesized
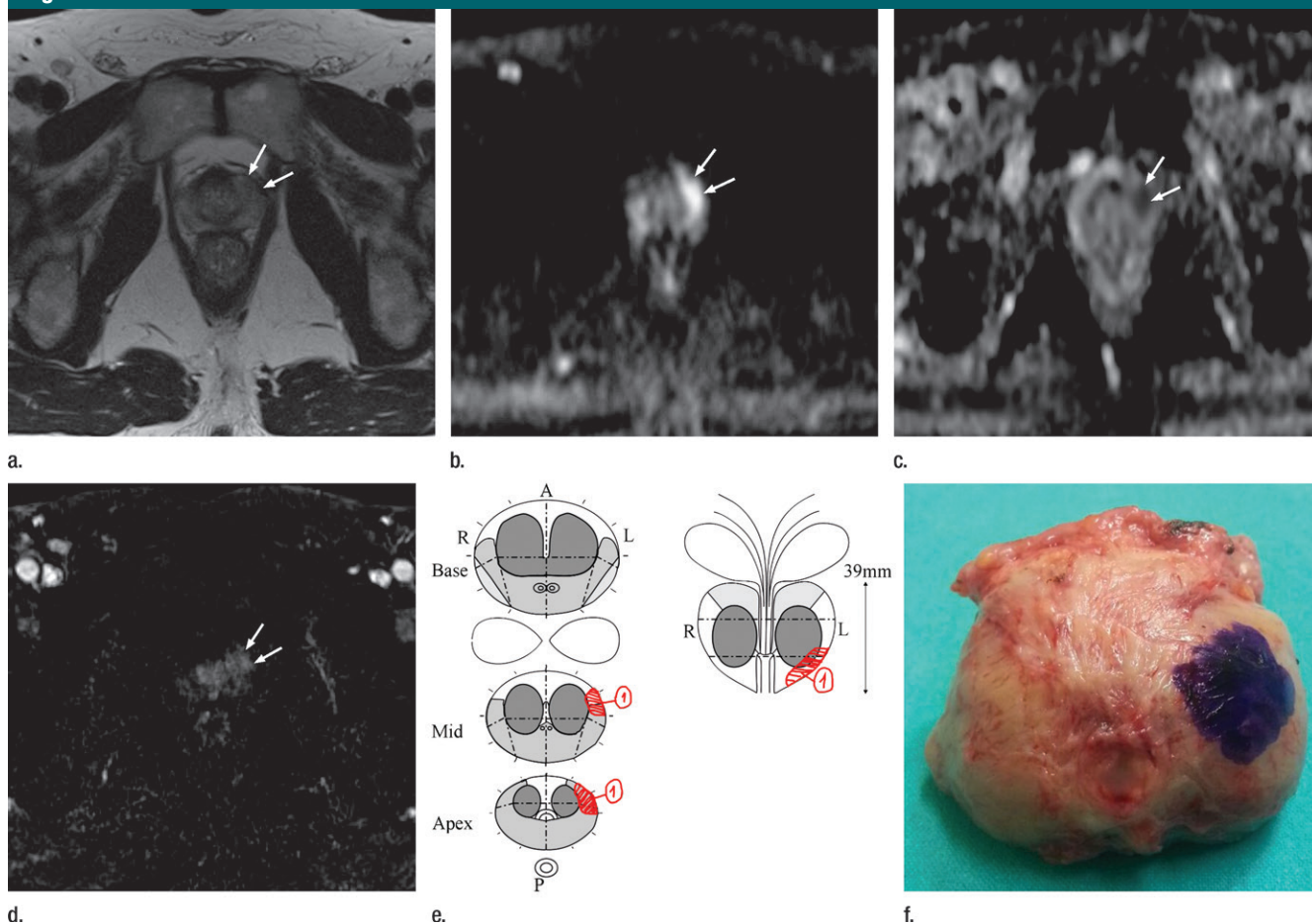
Figure 2

Figure 2: Illustration and images show process of preparation for multiparametric MR imaging–directed IFS during nerve-sparing RARP. Multiparametric MR image of the prostate shows an 11-mm lesion in the peripheral zone of anterolateral left aspect at midgland and apex levels. Lesion (arrows on **a-d**) was seen on **(a)** axial T2-weighted image as a slightly asymmetric area of lower signal intensity with mass effect on prostatic capsule (bulging), **(b)** on axial diffusion-weighted image with b value of 1000 sec/mm^2 as a focal mass of hyperintensity, **(c)** on apparent diffusion coefficient map with a reduced apparent diffusion coefficient, and **(d)** on axial dynamic contrast-enhanced MR image as a focal, asymmetric enhancement (rapid initial enhancement followed by washout). Lesion was assigned final Likert score of 5. **(e)** Illustration shows standardized reporting scheme manually drawn by a radiologist on the basis of multiparametric MR images. Line dividing anteroposterior aspects of prostate is defined according to references 19, 20. **(f)** Photograph shows the corresponding prostate surface marked (dark spot) to indicate tumor contact with prostatic capsule. IFS analysis was used to evaluate this site.

that the percentage of positive surgical margins would be 20% in the control patient group and 8% in the MR imaging and IFS patient group. At a significance level of .05, an 80% power for detecting a difference between the group proportions of 12% was achieved for group sizes of 131 control patients and 131 MR imaging and IFS patients.

Control patients were individually matched to MR imaging and IFS patients according to age, PSA level, and tumor stage by using the "greedy matching"

algorithm (34), with exact matching of groups for tumor stage. These matching variables, as well as nerve-sparing extent (monolateral or bilateral), surgeon, and Gleason score and prostate tumor stage at final pathologic examination were compared between the two groups by using the nonparametric Wilcoxon signed-rank test for continuous variables and the Bowker test of symmetry for categorical variables.

Our study end point was the difference between MR imaging and IFS patients and control patients in the

percentage of positive surgical margins after nerve-sparing RARP as determined at final pathologic examination. Percentages of positive surgical margins in each group were compared with the McNemar test, and percentages of positive surgical margins were compared for other possible predictors (ie, age, PSA level, tumor stage, Gleason score at biopsy, nerve-sparing extent, and surgeon) by using the Wilcoxon two-sample test for continuous variables and the χ^2 test for categorical variables. A multivariate conditional logistic

Table 2

Clinical and Pathologic Data for MR Imaging and IFS Patients and Control Patients

Variable	MR Imaging and IFS Patients	Control Patients	P Value
Age (y)	61.2 ± 6.1*	61.4 ± 5.9*	.55
PSA level (ng/mL)†	7.58 ± 5.53*	7.07 ± 3.19*	.94
Gleason score at biopsy			.30
≤6	82 (61)	96 (72)	
7	40 (30)	31 (23)	
≥8	12 (9)	7 (5)	
Extent of nerve sparing			.38
Right	24 (18)	32 (24)	
Left	29 (22)	27 (20)	
Bilateral	81 (60)	75 (56)	
Surgeon			.08
A	37 (28)	22 (16)	
B	37 (28)	34 (25)	
C	60 (45)	78 (58)	
Gleason score at final pathologic examination			.62
≤6	38 (28)	48 (36)	
7	81 (60)	71 (53)	
≥8	15 (11)	15 (11)	
pT stage			.17
2a	3 (2)	13 (10)	
2b	10 (7)	2 (1)	
2c	52 (39)	61 (46)	
3a	57 (43)	49 (37)	
3b	12 (9)	9 (7)	

Note.—Unless otherwise indicated, data are number of patients, with percentages in parentheses ($n = 134$).

* Data are means ± standard deviation.

† To convert to Systéme International units (micrograms per liter), multiply by 1.

regression model was then performed to assess the independent contribution of each variable for predicting positive surgical margins and to estimate the odds ratio, with 95% confidence intervals of positive surgical margin occurrence for MR imaging and IFS patients compared with those of control patients.

P values less than .05 were considered to indicate a significant difference. Statistical analyses were performed with software (SAS version 9.2; SAS Institute).

Results

Patient Population

Clinical-pathologic data for the MR imaging and IFS patients and control patients are detailed in Table 2. Eighty-eight (66%) MR imaging and IFS patients and their 88 matched control patients had stage 1 tumors, while the remaining 46 (34%) MR imaging and IFS patients and their 46 matched control patients had stage 2 tumors. The two groups were comparable according to age, PSA, Gleason score at biopsy, nerve-sparing extent, surgeon, and Gleason score and prostate tumor stage at final pathologic examination.

Control Patients

In 25 (18.7%) of the 134 control patients (one, pT2a; nine, pT2c; 12, pT3b; and three, pT3b) final pathologic results showed positive surgical margins; the remaining 109 (83.3%) control patients (12, pT2a; two, pT2b; 52, pT2c; 37, pT3a; and six, pT3b) had negative surgical margins at final pathologic examination.

MR Imaging and IFS Patients

In 10 (7.5%) of the 134 MR imaging and IFS patients (three, pT2c; and seven, pT3a) final pathologic results showed positive surgical margins; the remaining 124 (92.5%) MR imaging and IFS patients (three, pT2a; 10, pT2b; 49, pT2c; 50, pT3a; and 12, pT3b) had negative surgical margins at final pathologic examination.

In 18 MR imaging and IFS patients, multiparametric MR imaging–directed IFS analysis showed results that were positive for cancer at a total of 24 sites of tumor contact with the prostatic capsule (of the 37 sites indicated at multiparametric MR imaging), all of which were subjected to secondary resection (Fig 2). In four of these patients, the secondary resections were performed on tissues adjacent to anterior or anterolateral aspects of the gland only (Table 3), contributing to conversion into negative surgical margins in two patients. In 12 patients, secondary resections were performed only on lateral or posterolateral aspects involving a part of the neurovascular bundle, contributing to conversion into negative surgical margins at final pathologic examination for nine patients. In two patients, secondary resections were performed on both anterolateral and posterolateral aspects of the gland, contributing to conversion into negative surgical margins for both cases. Overall, final pathologic results showed negative surgical margins in 13 of the 18 patients with positive findings at multiparametric MR imaging–directed IFS analysis (one, pT2a; one, pT2b; five, pT2c; five, pT3a; and one, pT3b). In the remaining five patients (one, pT2c; and four, pT3a), positive surgical margins were found at final pathologic examination. In these five patients, positive surgical margins were found in contact with the site of IFS analysis, although in four of them, positive surgical margins were also found distant from the sites of IFS analysis.

Among the remaining 116 patients, multiparametric MR imaging showed no tumor contact with the prostatic

capsule in 31 patients, who, therefore did not undergo IFS analysis. Tumor contact with the prostatic capsule was shown in 85 patients, all of whom underwent IFS analyses (of 181 sites). The 31 patients who did not undergo IFS analysis showed negative surgical margins at final pathologic examination. The other 85 patients had negative IFS analysis, and thus, no secondary resection was performed, but at final pathologic examination, 80 had negative surgical margins and five had positive surgical margins (two, pT2c; and three, pT3a). In all five of these patients, positive surgical margins were present in contact with a site of IFS analysis, (involving lateral or posterolateral margins in two patients); although in two patients there were also positive surgical margins distant from the sites of IFS analysis (one apical and one basal site). The linear extension of positive surgical margins ranged from 0.5 to 5 mm. Overall, 111 (two, pT2a; nine, pT2b; 44, pT2c; 45, pT3a; and 11, pT3b) of the 116 MR imaging and IFS patients with no or negative IFS analysis had negative surgical margins at final pathologic examination (Fig 3).

Multiparametric MR imaging had a negative predictive value of 100% (95% confidence interval: 89%, 100%) for the presence of positive surgical margins at final pathologic examination; all 31 patients in whom multiparametric MR imaging showed no tumor contact with the prostatic capsule had negative surgical margins at final pathologic examination. Among the remaining 103 patients in whom multiparametric MR imaging showed tumor contact with the prostatic capsule, 10 had positive surgical margins at final pathologic examination, for a positive predictive value of 9.7% (95% confidence interval: 5.4%, 17%). The resulting sensitivity and specificity for positive surgical margins at final pathologic examination were of 100% and 25%, respectively.

Rates of Positive Surgical Margins between Groups

Positive surgical margins were found less frequently in MR imaging and IFS patients compared with age-, PSA level-,

Table 3

Locations of Positive Multiparametric MR Imaging-directed IFS Findings

Location	Apex	Apex and Midgland	Midgland	Midgland and Base	Base	Apex, Midgland, and Base	Total
Anterior	3	1	0	0	1	0	5
Anterolateral	2	0	0	0	0	0	2
Lateral	0	0	3	1	0	0	4
Posterolateral	1	5	1	2	1	4	14
Posterior	0	0	0	0	0	0	0
Total	6	6	4	3	2	4	25

Note.—Findings include 25 positive lesions in 18 patients.
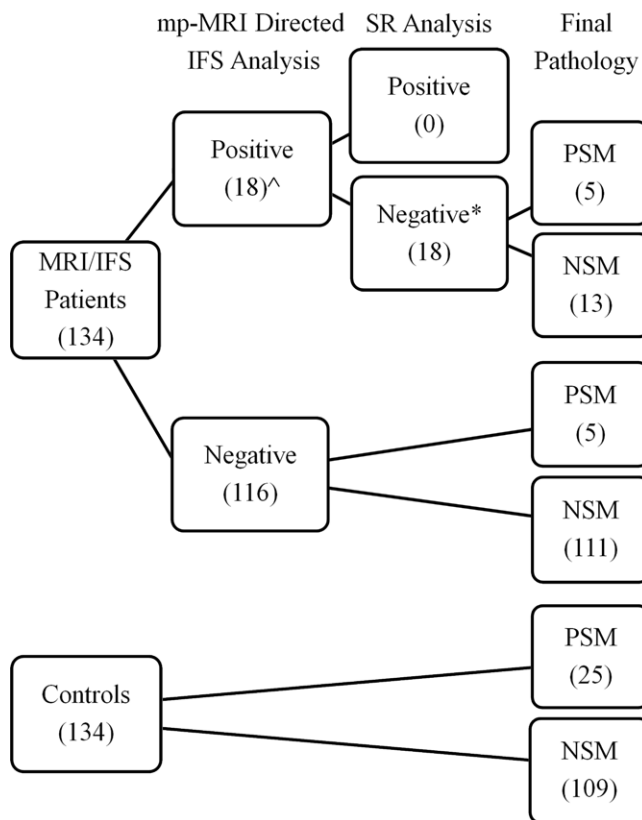
Figure 3

Figure 3: Diagram shows process of obtaining findings in patients who underwent multiparametric MR imaging–directed IFS analysis and at secondary resection (SR) and final pathologic examination. For comparison, final pathologic examination findings for control patients are also shown. PSM = positive surgical margin, NSM = negative surgical margin.

and stage-matched control patients (7.5% vs 18.7%, P = .01) (Table 4). In the multivariate analysis, the only significant predictor of positive margins was the group (MR imaging and IFS patients vs control patients), independent of other analyzed cofactors (Table 4). When the difference in risk factors was taken into account, MR imaging and IFS patients had one-seventh the

Table 4

Association of Patient and Tumor Characteristics with Surgical Margins at Final Pathologic Examination

Variable	Final Pathologic Result		P Value	
	Positive Surgical Margin	Negative Surgical Margin	Univariate Analysis	Multivariate Analysis*
Age (y)	61.9 ± 5.5	61.2 ± 6.1	.56	.39
PSA level (ng/mL)†	9.10 ± 7.59	7.06 ± 3.81	.03	.53
Gleason score at biopsy			.50	.14
≤6	21 (12)	157 (88)		
7	10 (14)	61 (86)		
≥8	4 (21)	15 (79)		
Tumor stage			>.99	NE
1	23 (13)	153 (87)		
2	12 (13)	80 (87)		
Multiparametric MR imaging–directed IFS			.007	.008
MR imaging and IFS patients	10 (7.5)	124 (92.5)		
Control patients	25 (18.7)	109 (81.3)		
Nerve-sparing side			.59	
Right	8 (14)	48 (86)		.66
Left	5 (9)	51 (91)		.41
Bilateral	22 (14)	134 (86)		Reference
Surgeon			.01	
A	8 (14)	51 (86)		.83
B	16 (23)	55 (77)		.09
C	11 (8)	127 (92)		Reference

Note.—Unless otherwise indicated, data are number of patients, with percentages in parentheses. NE = not estimable.

* Obtained from a conditional logistic regression model including the following independent possible predictive variables: age, PSA level, multiparametric MR imaging–directed IFS, Gleason score at biopsy, nerve-sparing side, and surgeon.

† To convert to Systéme International units (micrograms per liter), multiply by 1.

risk of having positive surgical margins relative to control patients (adjusted odds ratio: 0.15; 95% confidence interval: 0.04, 0.61).

In post hoc analyses of MR imaging and IFS patients according to pathologic stage, only patients with pT3 disease had a significant reduction in the risk of positive surgical margins compared with control patients (pT2: three of 65 [5%] vs 10 of 76 [13%], respectively; P = .08; pT3: seven of 69 [10%] vs 15 of 58 [26%], respectively; P = .02). Similarly, there was no significant difference in time between multiparametric MR imaging examination and nerve-sparing RARP between patients who had negative surgical margins and those with positive surgical margins at final pathologic examination (29 days ± 28 vs 26 days ± 25; P = .77).

Discussion

In 13 of the 18 MR imaging and IFS patients with positive results, secondary resection led to conversion into a prognostically more favorable negative surgical margin state at final pathologic examination. This is clinically relevant because biochemical recurrence-free survival has been reported not to differ between patients whose positive IFS results were converted to negative surgical margins at final pathologic examination and patients who had negative surgical margins without undergoing IFS (14).

The positive surgical margin rate seen in MR imaging and IFS patients (7.5%) was roughly half that reported in a recent large study of 11 069 patients describing IFS analysis at radical prostatectomy (15%) (14). Our lower positive surgical margin rate may be related to the added value of multiparametric MR imaging for detection and localization of clinically significant prostate cancers (larger volume, higher-grade index lesions), which are known to be responsible for most positive surgical margins (98.8%) (21). Our IFS analysis was directed by multiparametric MR imaging to the areas at highest risk for positive surgical margin. In one-third of our positive IFS patients (six of 18), multiparametric MR imaging directed the IFS analysis to the anterior or anterolateral aspects of the gland. These areas would likely not have been analyzed if IFS analysis was performed in the standardized areas of interest for nerve sparing (ie, the posterolateral aspects of the gland) (14). Moreover, the ability of multiparametric MR imaging–directed IFS analysis to provide timely, intraoperative confirmation of surgical margin status for anterior tumors may have application to newer surgical techniques such as complete anterior preservation (35).

Our approach is a change in strategy for the use of preoperative MR imaging. The standard use of preoperative MR imaging has been to assess extraprostatic tumor extension, with an extremely variable accuracy (50%–92%) (36). This sometimes poor performance of multiparametric MR imaging for depicting extraprostatic tumor extension has not hindered the surgical approach in routine clinical practice, particularly as surgeons have become more aggressive even in treating patients with established extracapsular extension of disease (15,22,37,38). The clinical emphasis has changed to achieving negative surgical margins at every operation. With our multiparametric MR imaging–directed approach, the assessment of extracapsular tumor extension and the related clinical decisions (eg, whether to resect the neurovascular bundle) were based on IFS histologic analysis. The role of multiparametric MR imaging was to identify sites for IFS analysis. The use of widely

available MR imaging equipment and IFS analysis may make our approach appealing for hospitals seeking to reduce positive surgical margin rates at robotic prostatectomy (39). We found that multiparametric MR imaging was excellent for ruling out tumor contact with the surface of the resected prostate; all 36 patients in whom multiparametric MR imaging indicated no tumor contact with the prostatic capsule had negative surgical margins at final pathologic examination (negative predictive value of 100%). This is consistent with results of prior studies on prostate tumor staging (22) and suggests that multiparametric MR imaging can be used to select patients in whom the IFS procedure can be avoided safely to save time instead of performing IFS analyses of standardized areas of the prostate in all patients. Furthermore, because all posterior lateral regions without multiparametric MR imaging–depicted tumor contact with the prostatic capsule had negative surgical margins, surgeons were able to plan operations more confidently and advise patients accordingly.

In 10 MR imaging and IFS patients (five positive and five negative), the final pathologic results showed positive surgical margins. In all 10 patients, there were positive surgical margins in contact with sites of multiparametric MR imaging–directed IFS analysis. This suggests that multiparametric MR imaging allowed correct location of the tumor contact but not always of its full extent, or that IFS analysis did not show the entire extent of multiparametric MR imaging findings. Although the completed graphical reporting scheme of the structured radiologic report (Fig 2) is thought to aid in communication, and thus, the targeting of IFS analysis, further improvements to avoid misinterpretation are desirable. The presence of positive surgical margins distant from sites of multiparametric MR imaging–directed IFS analyses in six of these 10 MR imaging and IFS patients (two pT2c and four pT3a) indicates a failure of the modality to allow identification of all tumor foci, and thus, to guide IFS

analysis in the presence of bilateral tumor involvement and/or extracapsular tumor extension that may include microscopic involvement of the bladder neck. However, in all these cases of positive surgical margins in multiparametric MR imaging and IFS patients, the contact of tumor cells with the surgical margin was small (< 5 mm), and so the effect on recurrence-free survival may be limited (14). Overall, multiparametric MR imaging had a relatively low positive predictive value (23.4%) for the presence of tumor on the resected prostate margin. In part, this reflects the limits of resolution of multiparametric MR imaging pulse sequences, as well as our practice of conservative reading, favoring a high negative predictive value (100%). There is a further possibility that the prostatic capsule, as visualized on MR images, is was misrepresented relative to the fascia plane followed by the surgeons during nerve-sparing RARP.

Because multiparametric MR imaging adds to the cost and complication of patient treatment, its inclusion in the presurgical routine must be fully justified. An important limitation of our study was that we cannot disentangle the separate contribution of multiparametric MR imaging and IFS in the achievement of lower positive surgical margin rates because we did not include a group of patients undergoing nerve-sparing RARP with IFS analysis without multiparametric MR imaging direction. Although we acknowledge the limitations of comparisons between studies, the positive surgical margin rate achieved in our MR imaging and IFS cohort (7.5%) compares favorably with results of recent reports (40,41), indicating that secondary resection based on IFS targeted to areas that the surgeon subjectively chooses or the entire prostate surface adjacent to the neurovascular bundle can result in positive surgical margins in nerve-sparing RARP of between 9.7% and 16%, respectively. We have also not examined the effect of multiparametric MR imaging–directed IFS analysis on clinical outcomes such as disease-free survival and functional recovery. Furthermore, we

have not attempted to evaluate the rate of unnecessary IFS performed on the basis of multiparametric MR imaging findings; pathologic evaluation of tumor focality for comparison with multiparametric MR imaging was not performed because this process was not expected to affect the study's primary endpoint. Selection of cases with a nonrandomized procedure may have resulted in differential selection bias (ie, patients may have presented specific characteristics associated with the outcome). Although nonrandomized distribution of unknown confounders between case and control patients could not be ruled out completely, we paid particular attention that case and control patients were similar for all the known characteristics associated with the outcome. We found that no known risk factor for positive margins was differently distributed in case and control patients.

In conclusion, significant reductions in positive surgical margin rates can be achieved in patients with prostate cancer who undergo nerve-sparing RARP by using multiparametric MR imaging–directed IFS analysis as shown in this case controlled study, which also provides encouraging preliminary evidence of the likely clinical benefit of this approach.

References

1. Montorsi F, Wilson TG, Rosen RC, et al. Best practices in robot-assisted radical prostatectomy: recommendations of the Pasadena Consensus Panel. Eur Urol 2012;62(3): 368–381.

2. Skarecky DW. Robotic-assisted radical prostatectomy after the first decade: surgical evolution or new paradigm. ISRN Urol 2013;2013:157379.

3. Ficarra V, Novara G, Ahlering TE, et al. Systematic review and meta-analysis of studies reporting potency rates after robot-assisted radical prostatectomy. Eur Urol 2012;62(3):418–430.

4. Tewari AK, Srivastava A, Huang MW, et al. Anatomical grades of nerve sparing: a risk-stratified approach to neural-hammock sparing during robot-assisted radical prostatectomy (RARP). BJU Int 2011;108(6 Pt 2):984–992.

5. Coelho RF, Chauhan S, Palmer KJ, Rocco B, Patel MB, Patel VR. Robotic-assisted radical prostatectomy: a review of current outcomes. BJU Int 2009;104(10):1428–1435.

6. Coelho RF, Rocco B, Patel MB, et al. Retropubic, laparoscopic, and robot-assisted radical prostatectomy: a critical review of outcomes reported by high-volume centers. J Endourol 2010;24(12):2003–2015.

7. Miller J, Smith A, Kouba E, Wallen E, Pruthi RS. Prospective evaluation of short-term impact and recovery of health related quality of life in men undergoing robotic assisted laparoscopic radical prostatectomy versus open radical prostatectomy. J Urol 2007;178(3 Pt 1):854–858; discussion 859.

8. Smith JA Jr, Chan RC, Chang SS, et al. A comparison of the incidence and location of positive surgical margins in robotic assisted laparoscopic radical prostatectomy and open retropubic radical prostatectomy. J Urol 2007;178(6):2385–2389; discussion 2389–2390.

9. Preston MA, Carrière M, Raju G, et al. The prognostic significance of capsular incision into tumor during radical prostatectomy. Eur Urol 2011;59(4):613–618.

10. von Bodman C, Brock M, Roghmann F, et al. Intraoperative frozen section of the prostate decreases positive margin rate while ensuring nerve sparing procedure during radical prostatectomy. J Urol 2013;190(2):515–520.

11. Lepor H, Kaci L. Role of intraoperative biopsies during radical retropubic prostatectomy. Urology 2004;63(3):499–502.

12. Gillitzer R, Thüroff C, Fandel T, et al. Intraoperative peripheral frozen sections do not significantly affect prognosis after nerve-sparing radical prostatectomy for prostate cancer. BJU Int 2011;107(5):755–759.

13. Heinrich E, Schön G, Schiefelbein F, Michel MS, Trojan L. Clinical impact of intraoperative frozen sections during nerve-sparing radical prostatectomy. World J Urol 2010;28(6):709–713.

14. Schlomm T, Tennstedt P, Huxhold C, et al. Neurovascular structure-adjacent frozen-section examination (NeuroSAFE) increases nerve-sparing frequency and reduces positive surgical margins in open and robot-assisted laparoscopic radical prostatectomy: experience after 11,069 consecutive patients. Eur Urol 2012;62(2):333–340.

15. Somford DM, Hamoen EH, Fütterer JJ, et al. The predictive value of endorectal 3 Tesla multiparametric magnetic resonance imaging for extraprostatic extension in patients with low, intermediate and high risk prostate cancer. J Urol 2013;190(5):1728–1734.

16. Hoeks CM, Barentsz JO, Hambrock T, et al. Prostate cancer: multiparametric MR imaging for detection, localization, and staging. Radiology 2011;261(1):46–66.

17. Sciarra A, Barentsz J, Bjartell A, et al. Advances in magnetic resonance imaging: how they are changing the management of prostate cancer. Eur Urol 2011;59(6):962–977.

18. Jung SI, Donati OF, Vargas HA, Goldman D, Hricak H, Akin O. Transition zone prostate cancer: incremental value of diffusion-weighted endorectal MR imaging in tumor detection and assessment of aggressiveness. Radiology 2013;269(2):493–503.

19. Seitz M, Shukla-Dave A, Bjartell A, et al. Functional magnetic resonance imaging in prostate cancer. Eur Urol 2009;55(4):801–814.

20. Arumainayagam N, Ahmed HU, Moore CM, et al. Multiparametric MR imaging for detection of clinically significant prostate cancer: a validation cohort study with transperineal template prostate mapping as the reference standard. Radiology 2013;268(3):761–769.

21. Karavitakis M, Ahmed HU, Abel PD, Hazell S, Winkler MH. Margin status after laparoscopic radical prostatectomy and the index lesion: implications for preoperative evaluation of tumor focality in prostate cancer. J Endourol 2012;26(5):503–508.

22. McClure TD, Margolis DJ, Reiter RE, et al. Use of MR imaging to determine preservation of the neurovascular bundles at robotic-assisted laparoscopic prostatectomy. Radiology 2012;262(3):874–883.

23. Padhani A. Integrating multiparametric prostate MRI into clinical practice. Cancer Imaging 2011;11(Spec No A):S27–S37.

24. Dickinson L, Ahmed HU, Allen C, et al. Magnetic resonance imaging for the detection, localisation, and characterisation of prostate cancer: recommendations from a European consensus meeting. Eur Urol 2011;59(4):477–494.

25. Hoeks CM, Hambrock T, Yakar D, et al. Transition zone prostate cancer: detection and localization with 3-T multiparametric MR imaging. Radiology 2013;266(1):207–217.

26. Jager GJ, Ruijter ET, van de Kaa CA, et al. Dynamic TurboFLASH subtraction technique for contrast-enhanced MR imaging of the prostate: correlation with histopathologic results. Radiology 1997;203(3):645–652.

27. Oto A, Kayhan A, Jiang Y, et al. Prostate cancer: differentiation of central gland cancer from benign prostatic hyperplasia by using diffusion-weighted and dynamic contrast-enhanced MR imaging. Radiology 2010;257(3):715–723.

28. Patel VR, Shah KK, Thaly RK, Lavery H. Robotic-assisted laparoscopic radical prostatectomy: the Ohio State University technique. J Robot Surg 2007;1(1):51–59.

29. Almeida GL, Musi G, Mazzoleni F, et al. Intraoperative frozen pathology during robot-assisted laparoscopic radical prostatectomy: can ALEXIS™ trocar make it easy and fast? J Endourol 2013;27(10):1213–1217.

30. Samaratunga H, Montironi R, True L, et al. International Society of Urological Pathology (ISUP) Consensus Conference on Handling and Staging of Radical Prostatectomy Specimens. Working group 1: specimen handling. Mod Pathol 2011;24(1):6–15.

31. Epstein JI, Allsbrook WC Jr, Amin MB, Egevad LL; ISUP Grading Committee. The 2005 International Society of Urological Pathology (ISUP) Consensus Conference on Gleason Grading of Prostatic Carcinoma. Am J Surg Pathol 2005;29(9):1228–1242.

32. UICC TNM Expert Panel. Prostate. In: Sobin LH, Gospodarowicz MK, Wittekind C, eds. TNM classification of malignant tumours. 7th ed. Chichester, England: Wiley-Blackwell, 2010; 243–248.

33. Tan PH, Cheng L, Srigley JR, et al. International Society of Urological Pathology (ISUP) Consensus Conference on Handling and Staging of Radical Prostatectomy Specimens. Working group 5: surgical margins. Mod Pathol 2011;24(1):48–57.

34. Bergstralh EJ, Kosanke JL, Jacobsen SJ. Software for optimal matching in observational studies. Epidemiology 1996;7(3):331–332.

35. Asimakopoulos AD, Annino F, D'Orazio A, et al. Complete periprostatic anatomy preservation during robot-assisted laparo-

scopic radical prostatectomy (RALP): the new pubovesical complex-sparing technique. Eur Urol 2010;58(3):407–417.

36. Heidenreich A. Consensus criteria for the use of magnetic resonance imaging in the diagnosis and staging of prostate cancer: not ready for routine use. Eur Urol 2011;59(4):495–497.

37. Roethke MC, Lichy MP, Kniess M, et al. Accuracy of preoperative endorectal MRI in predicting extracapsular extension and influence on neurovascular bundle sparing in rad-

ical prostatectomy. World J Urol 2013;31(5): 1111–1116.

38. Brown JA, Rodin DM, Harisinghani M, Dahl DM. Impact of preoperative endorectal MRI stage classification on neurovascular bundle sparing aggressiveness and the radical prostatectomy positive margin rate. Urol Oncol 2009;27(2):174–179.

39. Eastham JA, Kattan MW, Riedel E, et al. Variations among individual surgeons in the rate of positive surgical margins in

radical prostatectomy specimens. J Urol 2003;170(6 Pt 1):2292–2295.

40. Kakiuchi Y, Choy B, Gordetsky J, et al. Role of frozen section analysis of surgical margins during robot-assisted laparoscopic radical prostatectomy: a 2608-case experience. Hum Pathol 2013;44(8): 1556–1562.

41. Beyer B, Schlomm T, Tennstedt P, et al. A feasible and time-efficient adaptation of NeuroSAFE for da Vinci robot-assisted radical prostatectomy. Eur Urol 2014;66(1):138–144.